doi:10.1246/cl.2012.412
Published on the web April 4, 2012

Synthesis of PbS/EuS Core/Shell Nanocrystals

Takuya Nakashima,*[1] Hiroki Nakao,[1] Atsushi Tanaka,[1] Yasuchika Hasegawa,[1,2] and Tsuyoshi Kawai*[1]
[1]*Graduate School of Materials Science, Nara Institute of Science and Technology, 8916-5 Takayama, Ikoma, Nara 630-0192*
[2]*Division of Materials Chemistry, Graduate School of Engineering, Hokkaido University, N13 W8, Kita-ku, Sapporo, Hokkaiko 060-8628*

(Received January 17, 2012; CL-120039; E-mail: ntaku@ms.naist.jp, tkawai@ms.naist.jp)

The synthesis of nonmagnetic/magnetic PbS/EuS core/shell nanocrystals (NCs) has been demonstrated. PbS NCs were deposited by EuS layer via thermal decomposition of the single-source precursor, Eu(III)–dithiocarbamate complex, giving PbS/EuS core/shell NCs.

Semiconductor nanocrystals (NCs) have been attracting much attention for their optical, electric, and magnetic properties which can be modulated by a diverse and growing range of parameters such as size, shape, and composition unlike bulk semiconductors.[1] Recent interests focus on the preparation of semiconductor NCs with magnetic properties in anticipation of the use for spintronics as well as bioimaging. EuS NCs have been studied as a promising material because of the ferromagnetic Curie temperature, T_c, of 16.6 K, and characteristic magneto-optic properties in visible region.[2] Magnetic interactions in the self-assembling structures[3] or electron doping[4] have been reported to further enhance the magnetic properties of EuS NCs.

Another approach to enhance or modulate electric, optical, and magnetic properties of NCs may include the formation of hetero-nanostructures composed of multiple materials.[1,5] Recently, Scholes and co-workers have reported the integration of the magnetic semiconductor EuS NC with CdS NC to explore a bifunctional nanocomposite with a broken band alignment.[6] EuS–CdS heterostructures were synthesized via the selective deposition of EuS tips on cadmium chalcogenide NCs by the thermal decomposition of a single-source lanthanoid precursor. Our use of a heterostructure also aims to regulate and integrate the optical, magnetic, and magneto-optic properties of PbS/EuS heterostructure by means of the formation of a core/shell configuration. Since PbS has a rock-salt crystal structure whose lattice constant is very close to that of EuS with the lattice mismatch as low as 0.5%, PbS/EuS heterostructure has been studied as a nonmagnetic/magnetic all-semiconductor multilayers.[7,8] In PbS–EuS multilayers, wide-energy-gap EuS (E_g = 1.65 eV) form electron barriers, whereas narrow-energy-gap PbS (E_g = 0.3 eV) constitutes quantum wells for both electrons and holes.[8] Due to the relatively small energy difference in the valence band between PbS and EuS, 0.15 eV for bulk, together with the strong quantum confinement in PbS NCs[9] and the bulk properties of EuS NCs[2i] with Bohr radii of 20 nm and below 1 nm, respectively, there might be a possibility for the tuning of band offset through type I to type II by the size control of each component.[5] Given the type-II configuration, photogenerated electron and hole are expected to be localized separately in PbS and EuS, respectively. The spatially separated photocarriers lead to the long-lived exciton state, which might contribute to the enhancement of magneto-optic properties derived from magnetic exciton or magnetic polaron.[10–12]

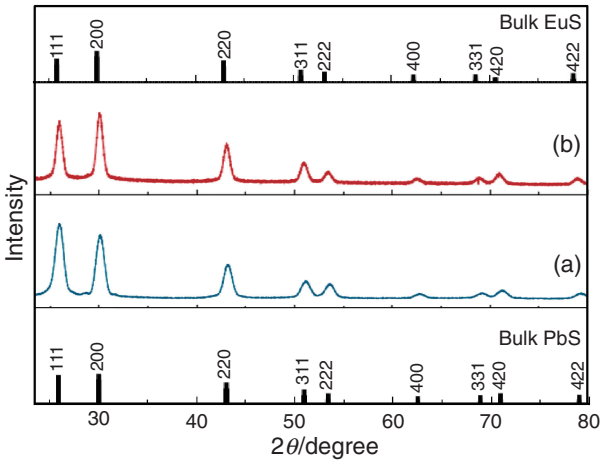

Figure 1. XRD profiles of (a) PbS NCs and (b) PbS/EuS core/shell NCs. The calculated peaks for PbS and EuS bulk crystals are indicated by lines at the bottom and the top, respectively.

PbS/EuS core/shell NCs were prepared by the deposition of EuS layer on PbS core NCs via the thermal decomposition of single-source Eu(III) precursor (see Supporting Information[17]). The powder X-ray diffraction (XRD) pattern for PbS core NCs suggested that the PbS crystallized in its typical rock-salt structure, cubic $Fm\bar{3}m$ phase (a = 5.924 Å) (Figure 1a). The peak positions 2θ of the diffraction pattern after the thermal decomposition of the single-source precursor of EuS were identical with those for PbS core NCs (Figure 1b) because the typical crystal structure of EuS is also cubic $Fm\bar{3}m$ phase with the lattice constant of a = 5.957 Å. The width of each peak sharpened after the deposition of EuS shell even though there is a nonzero lattice mismatch between these components. The single-crystal domain size of NCs calculated using Scherrer's equation from a diffraction peak (200) plane were found to be about 9 and 12 nm for PbS and PbS/EuS core/shell NCs, respectively, suggesting the epitaxial growth of EuS shell on the PbS core. Rounded cube-shaped NCs were observed in TEM image (Figure 2a), whose average size increased from 9.7 nm of PbS core NCs to 16.1 nm with a particle size distribution of 7%. The difference between the size of PbS/EuS core/shell NCs estimated by XRD and TEM might be attributed to the nonzero lattice mismatch which broadens the peaks and to the less crystalline oxidized layer of EuS surface, Eu_2O_3, as discussed later in detail. Elemental distribution was investigated for lead

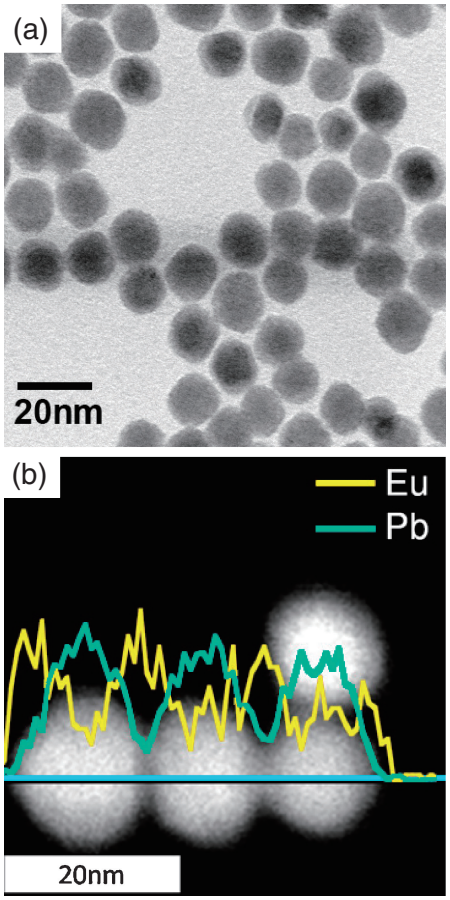

Figure 2. (a) TEM image and (b) HAADF-STEM image with an EDS-line analysis of PbS/EuS core/shell NCs.

and europium by high-angle annular dark-field scanning TEM energy-dispersive X-ray spectroscopy (HAADF-STEM-EDS). An EDS-line scan for a row of three horizontal NCs clearly shows that these elements are heterogeneously distributed. The peaks for Pb correspond to the center of NCs, while those for Eu are located on the outer part of NCs (Figure 2b). The result strongly supports that the NCs are composed of core/shell heterostructure with the Pb-rich central part and the Eu-rich outer layer.

The presence of Eu, Pb, and S was also confirmed by X-ray photoelectron spectroscopy (XPS). The selected regions for Eu 3d, 4d, O 1s, S 2p, and Pb 4f were measured in detail to evaluate the valence of europium ion. Only weak signals were observed for Eu^{2+} (3d and 4d), while strong peaks were found for Eu^{3+} (3d) as well as O 1s for as-prepared sample (Figure 3a). The peak positions for Eu^{3+} are well coincident with those observed for Eu_2O_3,[13] clearly indicating that the surface of NC was spontaneously oxidized upon exposure to air to form Eu_2O_3. The formation of amorphous Eu_2O_3 layer with the surface oxidation of EuS NCs was also reported by Gao and co-workers[2d] (also see Supporting Information[17]). To confirm the formation of EuS (Eu^{2+}), the oxidized surface Eu_2O_3 layer was removed by Ar-ion sputtering for a certain period. The peaks for Eu^{2+} (3d and 4d) became prominent as the specimen was subjected to the Ar-ion etching for several minutes, which was

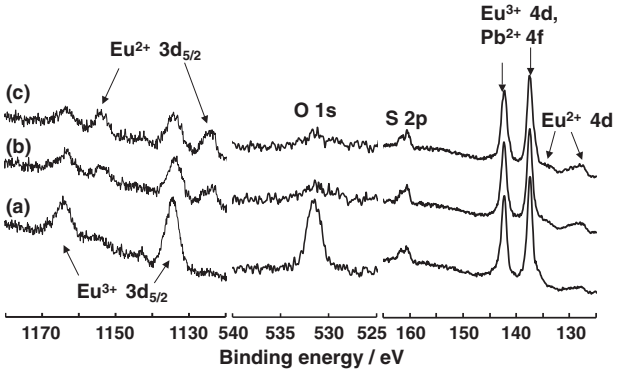

Figure 3. Core level spectra of Eu 3d, O 1s, S 2p, Eu 4d, and Pb 4f for PbS/EuS core/shell NCs. As-prepared sample (a) was subjected to Ar-ion etching for (b) 3 and (c) 6 min.

associated with the apparent decrease of the signal from O 1s (Figures 3b and 3c). Based on the size of NCs measured by TEM observation and the single-crystal domain size estimated from the XRD peak width, the PbS core (9 nm) was surrounded by the shell composed of 1.5-nm-thick crystalline EuS layer with the less crystalline Eu_2O_3 outer layer about 2-nm-thick. The element ratio of Pb/Eu determined by microwave-induced plasma mass spectrometer (MIP-MS) was 1/1, which is almost consistent with the model described above.

Absorption and magnetic circular dicroism (MCD) spectra of PbS core and PbS/EuS core/shell NCs are shown in Figure 4 together with those of EuS NCs with a diameter of 15 nm as reference. The PbS core NCs gave an absorption spectrum extended to near-infrared region with the weak first exciton peak at around 2000 nm in $CDCl_3$, which is well accorded with the calculated value for PbS NC with the size of 9 nm (Figure 4A, line a).[14] Because of the narrow band gap and consequent enhanced multiphonon nonradiative relaxation,[15] the PbS NCs exhibited no photoluminescence at room temperature. The absorption spectrum for PbS/EuS core/shell NCs seems mostly unchanged from that of PbS core NCs due to the small proportion of EuS layer only 1.5-nm-thick, while the f–d electronic transition band of Eu^{2+} should appear at around 500 nm as observed for 15-nm EuS NCs (Figure 4A, line c). Meanwhile the Eu_2O_3 shell, which accounts for the large portion of NC, had no impact on the absorption profile due to the markedly forbidden nature of the f–f transition of Eu^{3+} in Eu_2O_3.

Although there was little change in the absorption profile, the magnetic circular dichroism (MCD) spectrum clearly confirmed the formation and the spin-polarized semiconducting band of EuS shell. The peaks observed for MCD spectrum of PbS/EuS NCs (Figure 4B, line b) are corresponding to the electronic transition of $4f^7(^8S_{1/2}) \rightarrow 4f^6(^7F_J)5d(t_{2g})^1$ ($J = 0, \ldots, 6$) in the EuS component. Meanwhile, no obvious MCD signal was observed for PbS core-only NCs (Figure 4B, line a). The splitting of MCD signals with different directions corresponds to the difference in the transition probability for left- and right-hand circularly polarized light in the external magnetic field with 0.85 T. The MCD profile for PbS/EuS core/shell NCs showed a spin imbalance similar to that of EuS NCs (Figure 4B, line c), which is accompanied by substantial blue shift due to the

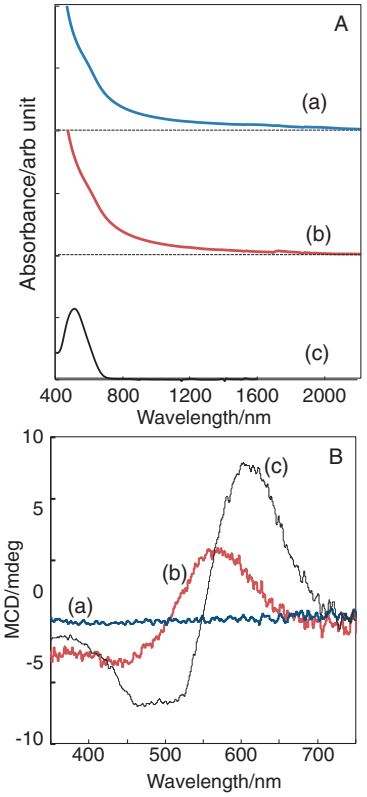

Figure 4. (A) Absorption (in $CDCl_3$) and (B) MCD (in $CHCl_3$) spectra of (a) PbS NCs, (b) PbS/EuS core/shell, and (c) EuS (size: 15 nm) NCs. In the MCD measurements, 0.85 T of magnetic field was applied statically in parallel to the optical axis.

size effect of EuS.[16] Thus the EuS component demonstrated magneto-optic properties of PbS/EuS core/shell NCs.

In summary, PbS/EuS core/shell NCs were synthesized via the thermal decomposition of single-source precursor of EuS on the core PbS NCs. The EDS-line scan of the NCs clearly demonstrated the core/shell configuration of the heterostructure, and XRD study indicated the epitaxial growth of EuS layer on the PbS core. Even though the EuS layer is 1.5-nm-thick due to the spontaneous surface oxidation, clear magneto-optical properties were demonstrated. The systematic study in terms of precise size control of the PbS core or the position and the width of band gap would give a great potential to modulate or enhance the magneto-optical properties of the PbS/EuS heterostructure.

The authors thank S. Fujita, Y. Kawai, and S. Katao for the assistance with TEM observation, Y. Okajima for XPS measurements, and M. Fujihara for MIP-MS analyses. This work was partly supported by a Grant-in-Aid for Scientific Research on Innovative Area "Emergence in Chemistry" (YH) from the Ministry of Education, Culture, Sports, Science and Technology (MEXT).

References and Notes

1 a) C. de Mello Donegá, *Chem. Soc. Rev.* **2011**, *40*, 1512. b) R. Costi, A. E. Saunders, U. Banin, *Angew. Chem., Int. Ed.* **2010**, *49*, 4878. c) G. D. Scholes, *Adv. Funct. Mater.* **2008**, *18*, 1157. d) T. Teranishi, M. Saruyama, M. Kanehara, *Nanoscale* **2009**, *1*, 225.
2 a) S. Thongchant, Y. Hasegawa, Y. Wada, S. Yanagida, *J. Phys. Chem. B* **2003**, *107*, 2193. b) T. Mirkovic, M. A. Hines, P. S. Nair, G. D. Scholes, *Chem. Mater.* **2005**, *17*, 3451. c) T. Kataoka, Y. Tsukahara, Y. Hasegawa, Y. Wada, *Chem. Commun.* **2005**, 6038. d) F. Zhao, H.-L. Sun, S. Gao, G. Su, *J. Mater. Chem.* **2005**, *15*, 4209. e) Y. Hasegawa, M. Afzaal, P. O'Brien, Y. Wada, S. Yanagida, *Chem. Commun.* **2005**, 242. f) F. Zhao, H.-L. Sun, G. Su, S. Gao, *Small* **2006**, *2*, 244. g) M. D. Regulacio, K. Bussmann, B. Lewis, S. L. Stoll, *J. Am. Chem. Soc.* **2006**, *128*, 11173. h) M. D. Regulacio, S. Kar, E. Zuniga, G. Wang, N. R. Dollahon, G. T. Yee, S. L. Stoll, *Chem. Mater.* **2008**, *20*, 3368. i) V. M. Huxter, T. Mirkovic, P. S. Nair, G. D. Scholes, *Adv. Mater.* **2008**, *20*, 2439.
3 a) A. Tanaka, H. Kamikubo, Y. Doi, Y. Hinatsu, M. Kataoka, T. Kawai, Y. Hasegawa, *Chem. Mater.* **2010**, *22*, 1776. b) A. Tanaka, H. Kamikubo, M. Kataoka, Y. Hasegawa, T. Kawai, *Langmuir* **2011**, *27*, 104.
4 a) S. Kar, W. L. Boncher, D. Olszewski, N. Dollahon, R. Ash, S. L. Stoll, *J. Am. Chem. Soc.* **2010**, *132*, 13960. b) R. S. Selinsky, J. H. Han, E. A. M. Pérez, I. A. Guzei, S. Jin, *J. Am. Chem. Soc.* **2010**, *132*, 15997.
5 Y. Nonoguchi, T. Nakashima, A. Tanaka, K. Miyabayashi, M. Miyake, T. Kawai, *Chem. Commun.* **2011**, *47*, 11270.
6 T. Mirkovic, D. Rossouw, G. A. Botton, G. D. Scholes, *Chem. Mater.* **2011**, *23*, 181.
7 T. Story, *Phys. Status Solidi B* **2003**, *236*, 310.
8 K. H. Aharonyan, *Physica E (Amsterdam, Neth.)* **2010**, *43*, 111.
9 F. W. Wise, *Acc. Chem. Res.* **2000**, *33*, 773.
10 T. Kasuya, A. Yanase, *Rev. Mod. Phys.* **1968**, *40*, 684.
11 P. Wachter, *CRC Crit. Rev. Solid State Sci.* **1972**, *3*, 189.
12 Y. Hasegawa, S. Thongchant, Y. Wada, H. Tanaka, T. Kawai, T. Sakata, H. Mori, S. Yanagida, *Angew. Chem., Int. Ed.* **2002**, *41*, 2073.
13 W.-D. Schneider, C. Laubschat, I. Nowik, G. Kaindl, *Phys. Rev. B* **1981**, *24*, 5422.
14 I. Kang, F. W. Wise, *J. Opt. Soc. Am. B* **1997**, *14*, 1632.
15 O. E. Semonin, J. C. Johnson, J. M. Luther, A. G. Midgett, A. J. Nozik, M. C. Beard, *J. Phys. Chem. Lett.* **2010**, *1*, 2445.
16 Y. Tsukahara, T. Kataoka, Y. Hasegawa, S. Kaizaki, Y. Wada, *J. Alloys Compd.* **2006**, *408–412*, 203.
17 Supporting Information is available electronically on the CSJ-Journal Web site, http://www.csj.jp/journals/chem-lett/index.html.

